Investigation of duty cycle controlled inductive wireless power transfer converter using series-series compensation for electric vehicle application

Bhavsingh Bhukya[1], Suresh Babu Gotluru[2], Mangu Bhukya[3], Ravi Kumar Bhukya[1], Vaani Dongari[1]
[1]Department of Electrical Engineering, Rajiv Gandhi University of Knowledge Technologies Basar, Nirmal, India
[2]Department of Electrical and Electronics Engineering, Chaitanya Bharathi Institute of Technology, Hyderabad, India
[3]Department of Electrical Engineering, University College of Engineering, Osmania University, Hyderabad, India

Article Info

Article history:

Received Mar 26, 2024
Revised Jul 12, 2024
Accepted Jul 17, 2024

Keywords:

Duty cycle control
Noncontact charging
Primary side control
Secondary side control
Series-series compensation

ABSTRACT

This paper presents series-series (SS) compensation topologies that include both primary side duty cycle control (PSDCC) and secondary side duty cycle control (SSDCC) methods. The main challenge for noncontact charging (NCC) for electric vehicles (EVs) batteries, the power transfer capability and efficiency in primary side proved to be unproductive. The investigation considers the primary side control duty cycle control (transmitter and receiver) and the secondary side duty cycle control (transmitter and receiver) in terms of compensation capacitor voltage, coil voltage, load side voltage, current, and power. By adjusting the duty cycle within the range of 0.1 to 0.5, it is possible to control power without significantly decreasing the system's efficiency, by using the SSDCC method. The evaluated parameters, including 1.5 kW output power, 85 kHz resonance frequency, and 120 mm ground clearance, are suitable for three-wheeler auto rickshaws. These findings are verified through MATLAB/Simulink software and compared with experimental results.

Corresponding Author:

Bhavsingh Bhukya
Department of Electrical Engineering, Rajiv Gandhi University of Knowledge Technologies Basar
Basar, Nirmal, Telangana, India
Email: bhavsingh.eee@rgukt.ac.in

1. INTRODUCTION

As compared to the internal combustion engine (IC Engine), the electric vehicle (EV) has more efficiency, lower operating and maintenance costs, less emission, and more comfort. The growth of EVs in the present promote could minimize the energy in transportation zone's dependence on fissile fuel. Though, a lot of challenges are taken from charging, traveling range, cost, and storage [1]. In that, the charging is the main consideration factor, to charge the battery for faster charging without any effect. In this regard, there is contact charging (CC) and noncontact charging (NCC). In CC, a lot of issues arise, those are increasing in the conductor size, safety concerns, and fast charging point of view the non NCC is the best method. NCC is the separation among the supply and charging as well as loads without any human requirements. In addition, NCC supports the medium and more power levels needed for excessive quick chargers, which significantly minimizes the charging time of the battery [2]–[8].

The basic method for controlling the output power in a NCC system involves the primary component of the load side voltage, current, and power to charge the battery for a faster range. Traditional duty-cycle control (TDC) is the constant control frequency method employed on the primary side cascaded converter [9]–[12] and secondary side bidirectional switches. In [13], the investigation of the control methods to study the zero voltage (ZVS) presentation of converters. In a NCC scheme to raise power capacity and minimize the charging of battery time, basically more power and frequency operations are forever needed to maintain the ZVS operation. Moreover, in the TDC method used in the primary side inverter, the td among the opposite switching illustrations of the converter phase-leg distorted the converter voltage and power. In [14], [15] investigation of converter considering the traditional phase shift pulse width modulation (PWM) method and evaluating its performance on the converter. The performance of the dead-time achieve is familiar in converter [16]. Performance of dead-time achieves in NCC appliances was addressed [17].

Kavimandan *et al.* [18] proposed a combination of frequency and conventional phase-shift method to moderate the voltage polarity reversal owing to the t_d. In view of the position cited beyond, an investigation of constant frequency duty cycle control methods on primary side and secondary side parameter variation such as parameter stress, output voltage, output current, and output power are neglecting in the text. Accordingly, in this paper focuses a specified mathematically performance of the duty cycle control on noncontact charging systems for the primary and secondary side PWM methods. The theoretical characterization of the converter and rectifier input waveforms for both side control techniques in view of the dead-time achieve is offered. At calculation, the performance of the td effect on the stresses on the parameter, output power and voltage as well as current at a particular duty cycle is conferred. A MATLAB model of the noncontact charging scheme is increased in MATLAB/Simulink to estimate and evaluate the achieves of the duty cycle control on both sides.

2. INTRODUCTION TO PRIMARY SIDE DUTY CYCLE CONTROL METHOD

Figure 1(a) employed the basic cascaded converter at fixed direct current (DC) voltage. Figure 1(b) represents the dead-time effect among the opposite switches to avoid the short circuit and switching losses. For the dead-time period, the switches are in zero position, and hence two metal–oxide–semiconductor field-effect transistors (MOSFETs) have enough time to clip among the turn on and off positions. Though, during the dead-time interval, if the current changes direction, the conduction of the switch modify the pole voltages of the converter, and accordingly, a mark arises at the converter [19]. Consequently, it is very significant to address the issue in the NCC system. The notch equation is defined as in (1).

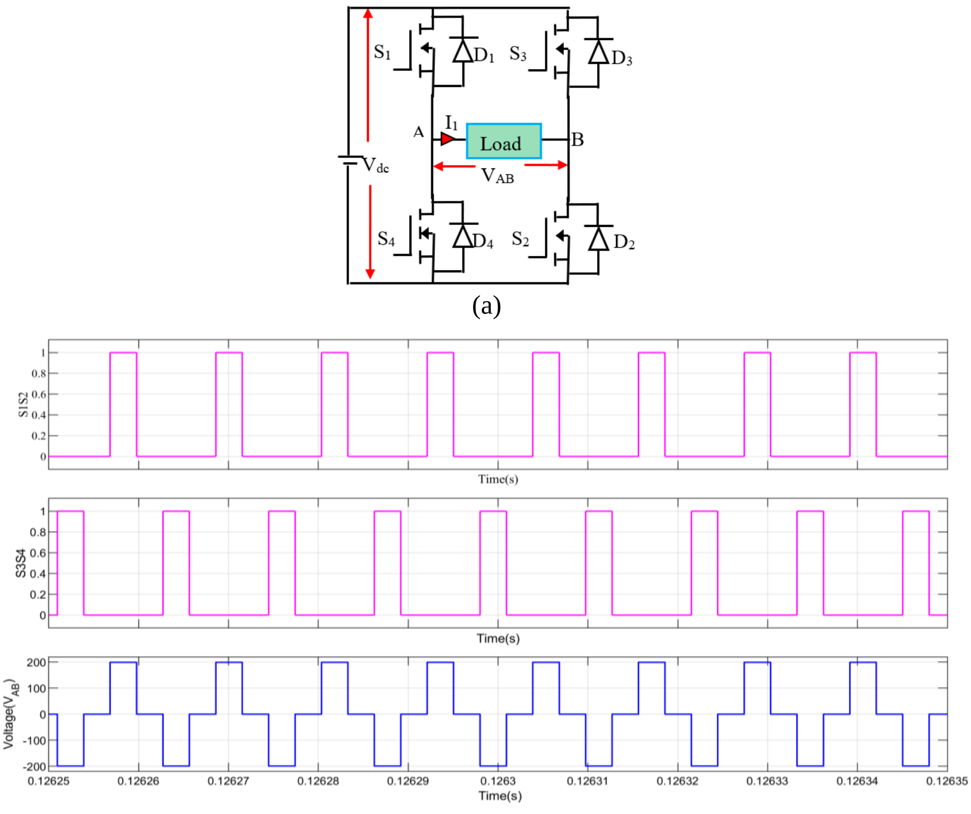

Figure 1. Basic H-bridge converter (a) basic circuit (b) pulses of the converter with t_d

$$|\theta_v - \varphi| \geq \frac{\psi_{td}}{2} \tag{1}$$

where φ is the fundamental component of converter current and voltage, θ_v angle among the converter fundamental component and output as well as ψ_{td} is the td angle given in (2). Where t_d is the dead-time in seconds and f is the switching frequency in Hz.

$$\psi_{td} = 2\pi \times f \times t_d \tag{2}$$

3. INTRODUCTION TO SECONDARY SIDE DUTY CYCLE CONTROL

Figure 2(a) shows the basic uncontrolled rectifier in front of the bidirectional switches, which is double the frequency presented and it is controlled to the output power very smoothly also it maintains the zero voltage (ZVS) switching at the inverter side [20]–[22]. As per the fundamental harmonic approximation (FHA) [23] in (3).

$$P_{out} = P_{in} = \mathrm{Re}(V_{AB} I_1^*) = \frac{1}{w_0 M} V_{AB} V_{CD} \tag{3}$$

where V_{AB} is the inverter output voltage, V_{CD} is the rectifier input voltage, w_0 is the resonance frequency, M is the mutual inductance and I_1 is the transmitter current can be written as in (4)

$$\mathrm{I_1} = \frac{\mathrm{V_{CD}}}{\mathrm{jw_0M}} = \frac{\mathrm{V_{CD}}}{\mathrm{jw_0M}} \angle 0^0 \tag{4}$$

From the waveform shown in Figure 2(b), the inverter voltage V_{AB} and rectifier input terminal voltage V_{CD} written in (5) and (6).

$$V_{AB} = \sum_{k=1}^{\infty} \frac{4}{(2k+1)\pi} V_{AB} sin\big((2k+1)w_0 t\big) \tag{5}$$

$$V_{CD} = \sum_{k=1}^{\infty} \frac{4}{-(2k+1)\pi} V_{CD} sin\left(\frac{2k+1}{2}(\pi - \alpha)\right) cos\big((2k+1)\big)w_0 t \tag{6}$$

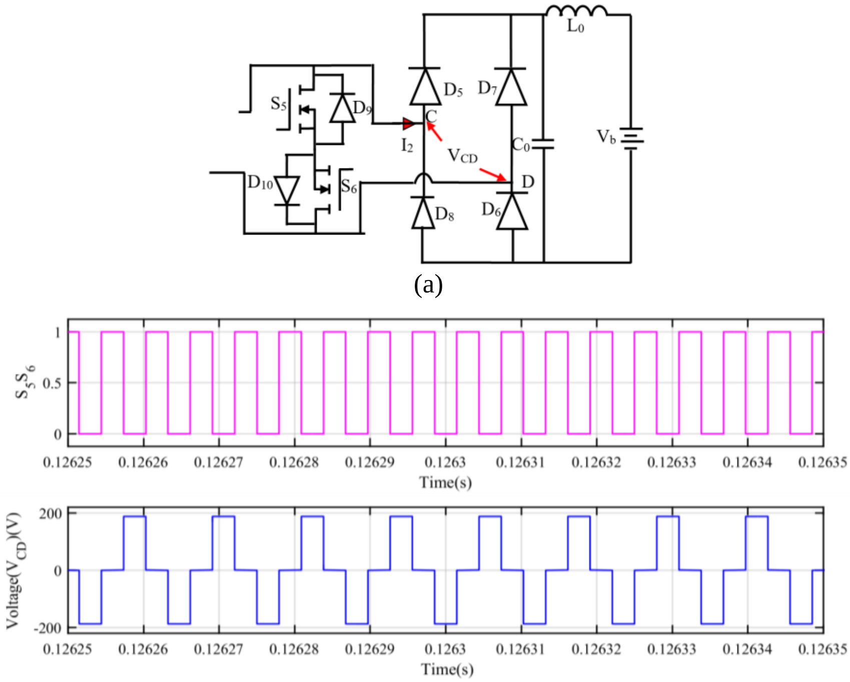

Figure 2. Secondary side bidirectional converter (a) switching circuit and (b) output voltage and switching pulses of the rectifier input circuit

Substituting V_{AB} and V_{CD} in P_{out} can also be written as in (7).

$$P_0 = \frac{V_{AB} \times V_{CD} \times 8}{\pi^2 w_0 M} \sum_{k=1}^{\infty} \frac{sin\left(\left(\frac{2k+1}{2}\right)\right)\pi(1-D)}{(2k+1)} \quad (7)$$

where D is the duty cycle, the output depends on the bidirectional switches of the duty cycle. By changing the duty cycle D the output voltage can be controlled without any disturbance on the primary side parameters and secondary side parameters. However, it does not require the secondary side additional DC-DC converter, the result is that the size and cost are reduced and the output is very smooth to achieve the zero-voltage switching at the transmitter side.

4. MATHEMATICALLY ANALYSIS OF A NCC METHOD

Figure 3(a) represents the basic schematic circuit of the series-series (SS) compensated NCC system [24], [25], and Figure 3(b) represents the FHA of the NCC system. Where L_1 and L_2 are the transmitter side and receiver side coil self-inductances, respectively; C_1 and C_2 are the secondary side and transmitter side capacitors, and R_1 and R_2 are the transmitter side coil and receiver side coil internal resistances. The AC equivalent resistance $Rac = \frac{8}{\pi^2} R_L$. By applying Kirchhoff's voltage law (KVL) in Figure 3(b), get the transmitter current and receiver currents is given as in (10) and (11).

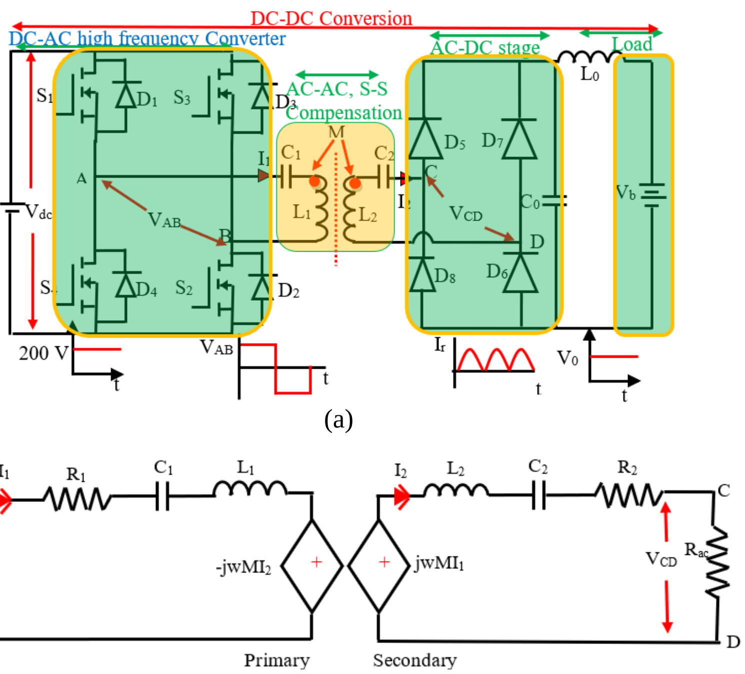

(a)

(b)

Figure 3. Schematic diagram of a NCC system (a) SS compensation and (b) first harmonic approximation of NCC system

$$V_{AB} = \left(R_1 + jwL_1 + \frac{1}{jwC_1}\right) l_1 - jwMl_2 \quad (8)$$

$$jwMl_1 = \left(R_2 + jwL_2 + \frac{1}{jwC_2}\right) l_2 + Racl_2 \quad (9)$$

$$I_1 = \frac{Z_2 V_{AB}}{Z_1 Z_2 + (wM)^2} \quad (10)$$

$$I_2 = \frac{jwMV_{AB}}{Z_1 Z_2 + (wM)^2} \quad (11)$$

Where, transmitter and receiver side impedances expressed as in (12) and (13).

$$Z_1 = R_1 + jwL_1 + \frac{1}{jwC_1} \quad (12)$$

$$Z_2 = R_2 + R_{ac} + jwL_2 + \frac{1}{jwC_2} \quad (13)$$

The frequency of the method is represented as in (14).

$${w_r}^2 = \frac{1}{L_1C_1} = \frac{1}{L_2C_2} \quad (14)$$

The response of the battery is represented as in (15) and (16).

$$P_{IN_{DC}} = V_{dc}I_{dc} \quad (15)$$

$$P_{OUT_{DC}} = I_2^2R_L \quad (16)$$

5. SIMULATION RESULTS AND DISCUSSION

5.1. Primary side duty cycle control method

Table 1 shows the coil structure and compensating capacitor modelled in MATLAB. The variation of the duty cycle at 0.5 along with a change in primary side parameters converter voltage, compensating capacitor voltage, and coil voltages are shown in Figure 4. Figure 4(a) shows the general waveform of the converter output voltage with the t_d achieves. Figures 4(b) and 4(c) shows the voltage across compensating capacitor and coil voltages. When the d is 0.5, the converter voltage (V_{AB}) and coil voltage V_t are more affected than the secondary side control methods, that discusses the secondary side duty cycle control method which is proposed in this paper for a better performance.

Table 1. Noncontact charging coils and parameters values

Components	Numbers
Transmitter capacitor/nF	10.79
Receiver capacitor/nF	7.4
Winding diameter	200 mm
L_1	325 µH
L_2	474.22 µH
d (air gap)	120 mm
M	62.8 µH
N_1	32
N_2	32
Coil	Circular
Frequency/kHz	85

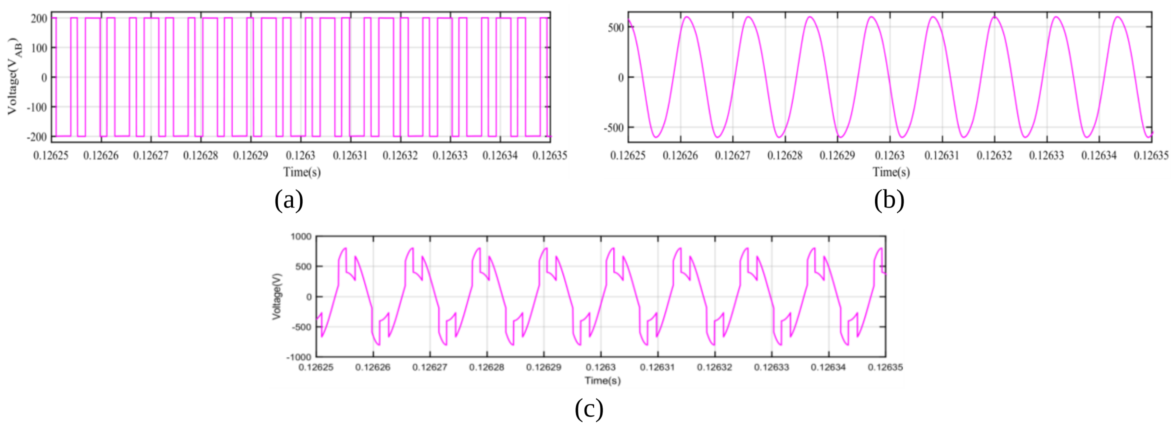

(a) (b) (c)

Figure 4. At duty cycle 0.5 (a) output voltage of the inverter (V_{AB}), (b) transmitter side capacitor voltage (V_{ct}) and (c) transmitter coil voltage (V_t)

The variation of the duty cycle at 0.5 along with a change in load side parameters rectifier input voltage, compensating capacitor voltage, coil voltages, and battery performance are shown in Figure 5. Figures 5(a) to 5(c) of the secondary side parameter voltages are less stressed as compared to the secondary side duty cycle control method. However, the battery performance which is very poor in the primary side control methods in Figures 5(d) to 5(g).

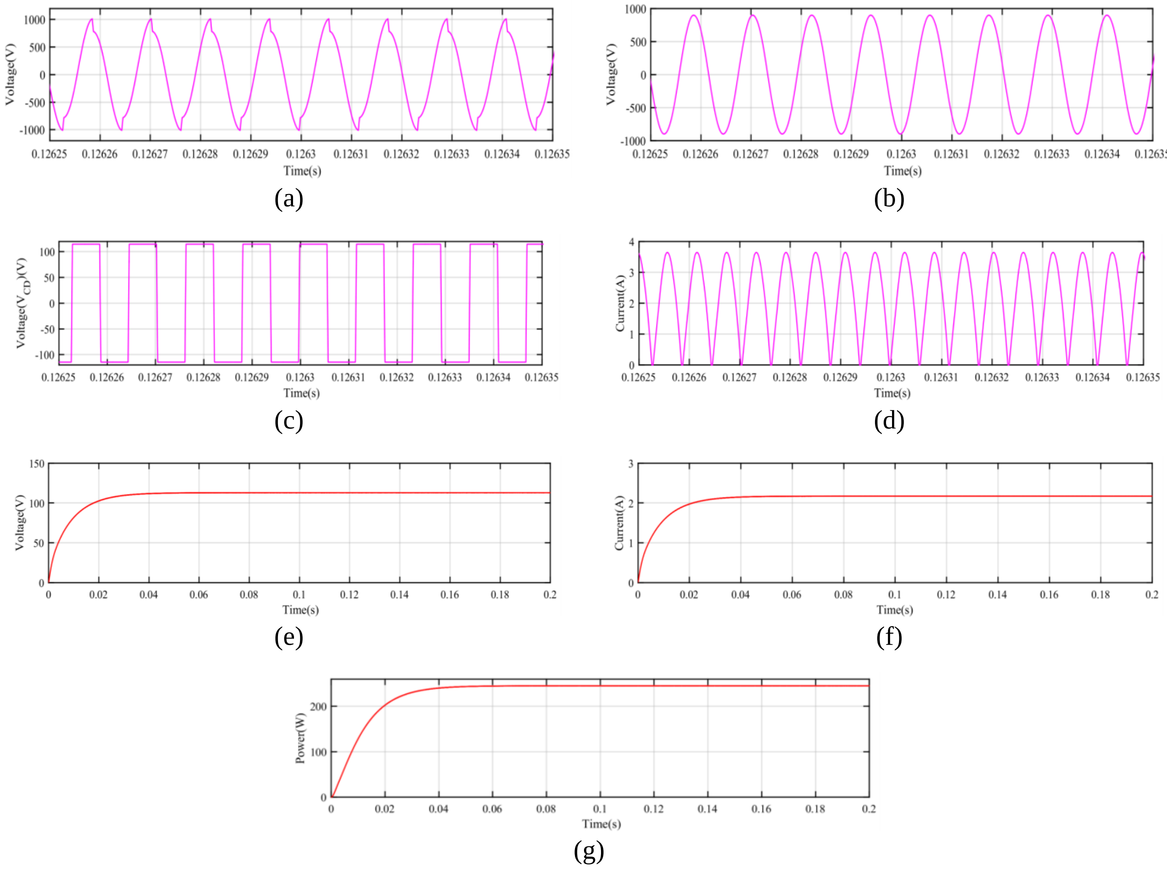

Figure 5. d= 0.5 (a) receiver coil voltage (V_r), (b) receiver side capacitor voltage (V_{cr}), (c) input voltage of the rectifier (V_{CD}), (d) rectifier output current, (e) load voltage (V_0), (f) load current (I_0), and (g) load power

5.2. Secondary side duty cycle control method

The variation of the duty cycle at 0.5 along with a change in primary side parameters inverter voltage, compensating capacitor voltage, and coil voltages are shown in Figure 6. Figure 6(a) shows the general waveform of the inverter output voltage without any td effect. Figures 6(b) and 6(c) shows the voltage across compensating capacitor and coil voltages. When the duty cycle is 0.5, the inverter voltage (V_{AB}) and coil voltage V_t are much smoother as compared to the primary side duty cycle control methods, that discusses the primary side duty cycle control method in this paper.

The deviation of the d at 0.5 along with a change in load side parameters rectifier input voltage, compensating capacitor voltage, coil voltages, and battery performance are shown in Figure 7. Figures 7(a), 7(b), and 7(c) of the secondary side parameter voltages are a little more stressed as compared to the primary side duty cycle control method. However, the battery performance is very effective, and smoother waveforms in the secondary side duty cycle control methods in Figures 7(d) to 7(g).

5.3. Comparison between primary side and secondary side duty cycle control methods

Figure 8 observed power of the secondary side duty cycle control (SSDCC) S-S compensation system duty cycle from 0.1 to 0.5 is more as compared to the primary side duty cycle control (PSDCC) method. It observed that it is sufficient to manage the power by changing the duty cycle within a limit (0.1≤0.5) as well and the efficiency of the system does not decrease significantly. In the process of the duty cycle increase 0.1 to 0.5, the system output power increases 0.02568 W to 245.1 W in the primary side control method as well as 41.4 W to 778.2 W in the secondary side duty cycle control method. Similarly, the power transfer efficiency is higher in the SSDCC method.

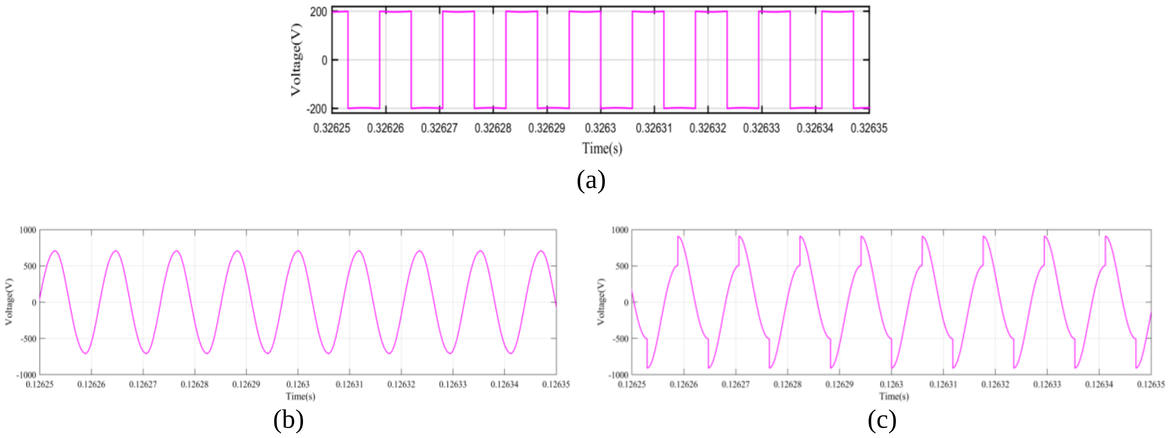

Figure 6. At d= 0.5 (a) output voltage of the inverter (V_{AB}), (b) transmitter side capacitor voltage (V_{ct}) and (c) transmitter coil voltage (V_t)

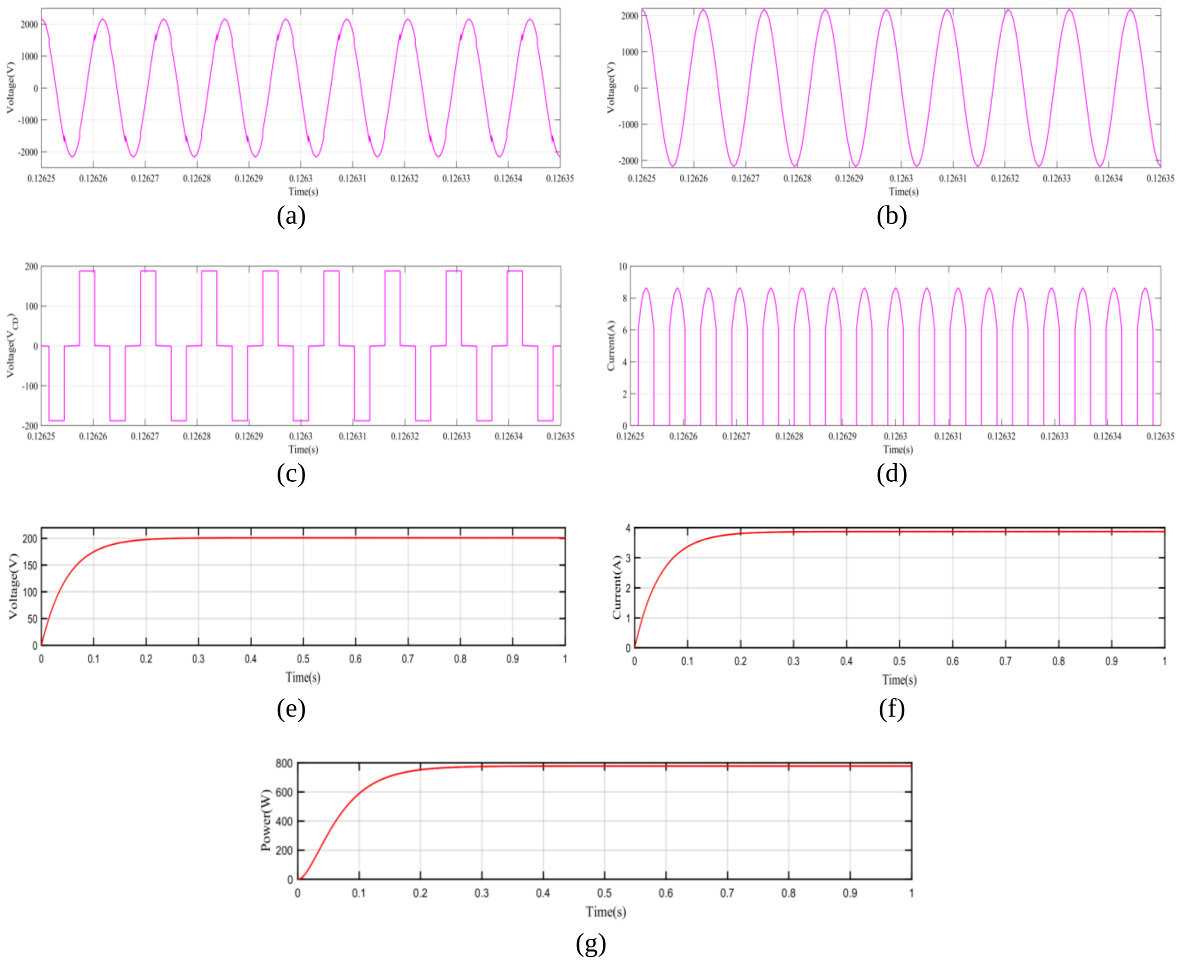

Figure 7. At duty cycle 0.5 (a) receiver coil voltage (V_r), (b) receiver side capacitor voltage (V_{cr}), (c) input voltage of the rectifier (V_{CD}), (d) rectifier output current, (e) load voltage (V_0), (f) load current (I_0), and (g) load power (P_0)

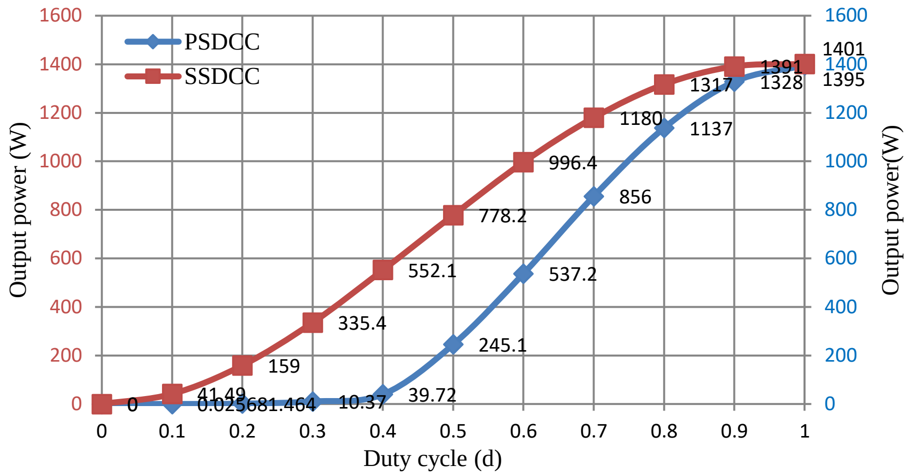

Figure 8. Comparison between primary side and secondary side duty cycle control methods

6. EXPERIMENTAL RESULTS AND DISCUSSION

A laboratory prototype of the NCC system with the SS method and the advised control scheme has been built to confirm the mathematical performance employed in Figure 9(a) (in appendix). Figure 9(b) (in appendix) shows the inverter gate pulses for switches S_1S_2 and S_3S_4. Figure 9(c) (in appendix) shows the transmitter current waveform flowing through inverter switches. Figure 9(d) (in appendix) shows the inverter output terminal voltage experimental results of the waveforms.

7. CONCLUSION

In giving the best output for the smooth functioning of EVs comparatively with that of existing vehicles, the SSDCC method (transmitter and receiver) for a NCC system with S-S (series-series) topology has been experimentally proven at the laboratory level as the best. The validity of evaluated parameters is checked through MATLAB/Simulink and compared with experimental results productively. The Comparison of voltage and current stresses on coils, compensating capacitors, and switches has been proven with the help of simulation studies. Thus, it is observed that the output power of the EVs battery in the PSDCC control method which is 0.1 to 0.5 proved to be very weak and less productive when compared to the SSDCC method. All this process and procedure has been discussed in detail in the figures and experimental diagrams for the clear understanding of this proposed phenomenon.

APPENDIX

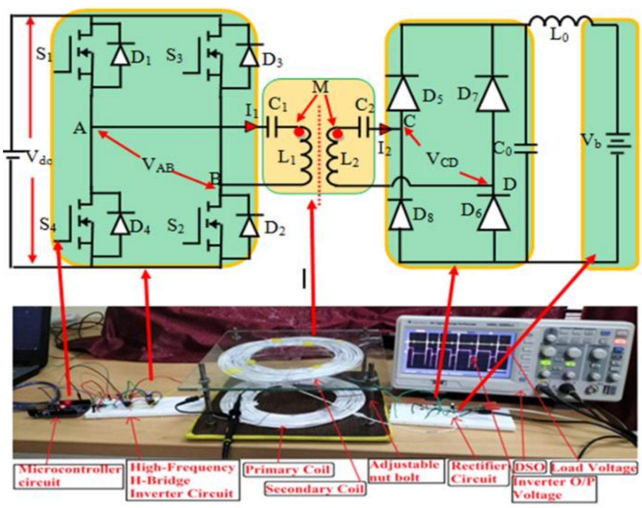

(a)

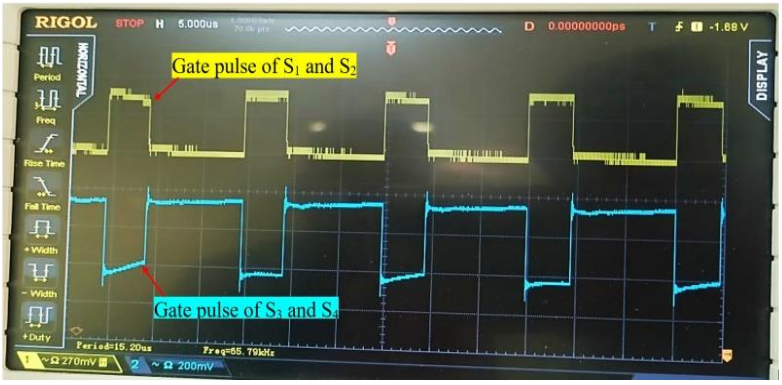

(b)

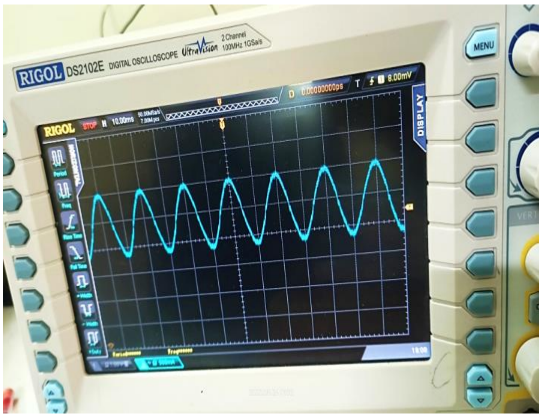

(c)

(d)

Figure 9. The hardware results of the waveforms (a) experimental proto type, (b) gate pulses, (c) transmitter current, and (d) inverter voltage

ACKNOWLEDGEMENTS

The authors are thankful to the Department of Electrical Engineering, Rajiv Gandhi University of Knowledge Technologies (RGUKT) Basar, for providing financial and technical support.

REFERENCES

[1] T. Omie Gogo and D. Zhu, “Analytical modelling with experimental validation of electromagnetic Halbach arrays in wireless power transfer systems,” *IET Microwaves, Antennas and Propagation*, vol. 18, no. 5, pp. 342–355, 2024, doi: 10.1049/mia2.12460.

[2] X. He *et al.*, “Wireless power and information dual transfer system via magnetically coupled resonators,” *Communications Engineering*, vol. 3, no. 1, pp. 1–12, 2024, doi: 10.1038/s44172-023-00154-4.

[3] Bozhi *et al.*, “A review of wireless pavement system based on the inductive power transfer in electric vehicles,” *Sustainability*, vol. 15, no. 20, 2023, doi: 10.3390/su152014893.

[4] K. Balamurugan, T. Janani, R. Keerthana, and S. J. Reshma, “Wireless charger for electric vehicles,” in *Proceedings of the International Conference on Intelligent Technologies in Security and Privacy for Wireless Communication, ITSPWC 2022, 14-15 May 2022, Karur, Tamilnadu, India*, 2022, no. February, doi: 10.4108/eai.14-5-2022.2318881.

[5] K. Yamaguchi, R. Okamura, H. Terada, and K. Iida, “Experimental review of an improving system on wireless power transfer via auto tuning of frequency,” *International Journal of Electrical and Computer Engineering*, vol. 13, no. 2, pp. 1314–1319, Apr. 2023, doi: 10.11591/ijece.v13i2.pp1314-1319.

[6] T. S. Pham, X. K. Bui, S. T. Bui, T. H. H. Le, and D. L. Vu, “A critical review on wireless power transfer systems using metamaterials,” *Vietnam Journal of Science and Technology*, vol. 60, no. 4, pp. 587–613, Aug. 2022, doi: 10.15625/2525-2518/16954.

[7] A. O. Elmeligy, E. Elghanam, M. S. Hassan, A. H. Osman, A. A. Shalaby, and M. Shaaban, “Optimal planning of dynamic wireless charging infrastructure for electric vehicles,” *IEEE Access*, vol. 12, no. March, pp. 30661–30673, 2024, doi: 10.1109/ACCESS.2024.3365636.

[8] N. T. Diep, T. D. Hiep, and N. K. Trung, “Constant current charging and transfer efficiency improvements for a dynamic wireless charging system,” *Engineering, Technology and Applied Science Research*, vol. 13, no. 6, pp. 12320–12326, 2023, doi: 10.48084/etasr.6315.

[9] Y. Xie *et al.*, “Research on the multiple capacitor current sharing of high-current receiving coils in a series – series wireless

charging system," *World Electric Vehicle Journal*, vol. 15, no. 2, Feb. 2024, doi: 10.3390/wevj15020058.
[10] P. K. Jain, A. St-Martin, and G. Edwards, "Asymmetrical pulse-width-modulated resonant DC/DC converter topologies," *IEEE Transactions on Power Electronics*, vol. 11, no. 3, pp. 413–422, 1996, doi: 10.1109/63.491634.
[11] J. A. Sabate and F. C. Lee, "Off-line application of the fixed frequency clamped mode series-resonant converter," in *Proceedings, Fourth Annual IEEE Applied Power Electronics Conference and Exposition*, 1991, pp. 213–220, doi: 10.1109/APEC.1989.36973.
[12] U. D. Kavimandan, V. P. Galigekere, O. Onar, B. Ozpineci, and S. M. Mahajan, "Comparison of dead-time effects in a WPT system inverter for different fixed-frequency modulation techniques," in *2020 IEEE Transportation Electrification Conference & Expo (ITEC)*, Jun. 2020, pp. 277–283, doi: 10.1109/ITEC48692.2020.9161646.
[13] F. Monterde, J. M. Burdio, P. Hernandez, and J. R. Garcia, "Unipolar voltage-cancellation control of resonant inverters for induction cooking appliances," in *IECON '98. Proceedings of the 24th Annual Conference of the IEEE Industrial Electronics Society (Cat. No.98CH36200)*, 1998, vol. 2, pp. 820–824, doi: 10.1109/IECON.1998.724199.
[14] K. Aditya and S. S. Williamson, "Comparative study on primary side control strategies for series-series compensated inductive power transfer system," in *2016 IEEE 25th International Symposium on Industrial Electronics (ISIE)*, Jun. 2016, pp. 811–816, doi: 10.1109/ISIE.2016.7744994.
[15] S. Bai, Z. Pantic, and S. Lukic, "A comparison study of control strategies for ZVS resonant converters," in *IECON 2010 - 36th Annual Conference on IEEE Industrial Electronics Society*, Nov. 2010, vol. 1, pp. 256–262, doi: 10.1109/IECON.2010.5675019.
[16] M. Vinod, D. Kishan, R. Kannan, A. Iqbal, and S. M. Sulthan, "Primary side control strategies for battery charging regulation in wireless power transfer systems for EV applications," *IET Power Electronics*, vol. 17, no. 8, pp. 941–952, Jun. 2024, doi: 10.1049/pel2.12639.
[17] J. M. Burdio, F. Canales, P. M. Barbosa, and F. C. Lee, "Comparison study of fixed-frequency control strategies for ZVS DC/DC series resonant converters," in *2001 IEEE 32nd Annual Power Electronics Specialists Conference (IEEE Cat. No.01CH37230)*, 2001, vol. 1, pp. 427–432, doi: 10.1109/PESC.2001.954057.
[18] U. D. Kavimandan, V. P. Galigekere, B. Ozpineci, and O. Onar, "Analysis of dead-time in a single phase wireless power transfer system," in *2019 IEEE Transportation Electrification Conference and Expo (ITEC)*, Jun. 2019, pp. 1–8, doi: 10.1109/ITEC.2019.8790467.
[19] X. Liu *et al.*, "Analysis and elimination of dead-time effect in wireless power transfer system," *Energies*, vol. 11, no. 6, Jun. 2018, doi: 10.3390/en11061577.
[20] U. D. Kavimandan, V. P. Galigekere, O. Onar, B. Ozpineci, and S. M. Mahajan, "A control scheme to mitigate the dead-time effects in a wireless power transfer system," in *2020 IEEE Applied Power Electronics Conference and Exposition (APEC)*, Mar. 2020, pp. 3172–3179, doi: 10.1109/APEC39645.2020.9124590.
[21] G. Feng, Z. Liu, X. Wei, Z. Liu, X. Zhu, and S. Shao, "Study of double-sided LCC compensation wireless power transfer based on zero voltage switching," in *2020 IEEE 3rd Student Conference on Electrical Machines and Systems (SCEMS)*, Dec. 2020, pp. 713–717, doi: 10.1109/SCEMS48876.2020.9352358.
[22] C. Cui, D. Pehrman, Y. Liu, and Q. Zhang, "Zero voltage switching for high power three-phase inductive power transfer with a dual active bridge," *IEEE Access*, vol. 12, no. December 2023, pp. 7121–7133, 2024, doi: 10.1109/ACCESS.2024.3351811.
[23] B. Pang, J. Deng, P. Liu, and Z. Wang, "Secondary-side power control method for double-side LCC compensation topology in wireless EV charger application," in *IECON 2017 - 43rd Annual Conference of the IEEE Industrial Electronics Society*, Oct. 2017, pp. 7860–7865, doi: 10.1109/IECON.2017.8217377.
[24] A. A. S. Mohamed, A. A. Shaier, H. Metwally, and S. I. Selem, "Wireless charging technologies for electric vehicles: inductive, capacitive, and magnetic gear," *IET Power Electronics*, no. May, pp. 1–27, Dec. 2023, doi: 10.1049/pel2.12624.
[25] S. Kuo *et al.*, "A review of wireless pavement system based on the inductive power transfer in electric vehicles," *Energies*, vol. 17, no. 2, Jan. 2024, doi: 10.3390/en17020354.

BIOGRAPHIES OF AUTHORS

Bhavsingh Bhukya is an assistant professor in the Department of Electrical and Electronic Engineering, RGUKT-IIIT, Basara, Telangana, India. He Obtained B.Tech. in electrical and electronics engineering from Vaagdevi College of Engineering, Warangal in 2009 and M.Tech. in power electronics in 2012 from Vaagdevi College of Engineering Warangal. He pursuing Ph.D. in Department of Electrical Engineering, University College of Engineering, Osmania University, and Hyderabad, India. His research interests include power electronics, DC-DC converters, electrical vehicles, and wireless transmission. He has more than 5 publications in international journals and has attended and presented papers in national conferences. He can be contacted at email: bhavsingh.eee@rgukt.ac.in.

Suresh Babu Gotluru is a professor of electrical engineering at the Department of Electrical and Electronics Engineering and Chaitanya Bharathi Institute of Technology (CBIT), Hyderabad. He received Ph.D. in 2013 and a master's degree in electrical engineering from Osmania University, Hyderabad, in 2001. His research interest is electric drives, energy management, and renewable energy. He can be contacted at: gsureshbabu_eee@cbit.ac.in.

Mangu Bhukya is a professor of electrical engineering at the Department of Electrical Engineering and Process, University College of Engineering, Osmania University, Hyderabad. He received Ph.D. in 2016 from IIT Bombay and a master's degree in electrical engineering from University College of Engineering (OU), in 2002. His research interest is renewable energy, electric vehicles, and power electronics converters. He can be contacted at email: mangu.b@uceou.edu.

Ravi Kumar Bhukya is a guest faculty in the Department of Electrical and Electronic Engineering, RGUKT-IIIT, Basara, Telangana, India. He obtained B.Tech. in electrical and electronics engineering from JNTUH in 2010 and M.Tech. in power and industrial drives in 2013 from JNTUH. He received Ph.D. in 2023 from Department of Electrical Engineering, University College of Engineering**,** Osmania University, and Hyderabad, India. His research interests include power electronics, drives, power converters, multi-level inverter, EV, wireless transmission, and special machines. He has more than 10 publications in international journals and has attended and presented papers in 6 national conferences. He can be contacted at email: ravikumarb.phd@uceou.edu.

Vaani Dongari is a guest lab assistant in the Department of Electrical and Electronic Engineering, RGUKT-IIIT, Basara, Telangana, India. He Obtained B.Tech. in electrical and electronics engineering from Nigam Engineering college, Karimnagar in 2012and M.Tech. in power electronics in 2014 from Vaagdevi College of Engineering Warangal. Her research interests include power electronics, electrical vehicles, and wireless transmission. She has two publications in international journals and has attended and presented papers in national conferences. She can be contacted at: dvani2020@gmail.com.